Russell Lecture: Dark Star Formation and Cooling Instability

D. Lynden-Bell[1]

Institute of Astronomy, The Observatories, Madingley Road, Cambridge, CB3 0HA, UK

dlb@ast.cam.ac.uk

and

C. A. Tout[2]

Institute of Astronomy, The Observatories, Madingley Road, Cambridge, CB3 0HA, UK

cat@ast.cam.ac.uk

Received _____; accepted _____

[1]and Clare College, Cambridge, UK

[2]and Churchill College, Cambridge, UK

ABSTRACT

Optically thin cooling gas at most temperatures above 30K will make condensations by pressure pushing material into cool dense regions. This works without gravity. Cooling condensations will flatten and become planar/similarity solutions. Most star formation may start from cooling condensations - with gravity only important in the later stages. The idea that some of the dark matter could be pristine white dwarfs that condensed slowly on to planetary sized seeds without firing nuclear reactions is found lacking. However, recent observations indicate fifty times more halo white dwarfs than have been previously acknowledged; enough to make the halo fraction observed as MACHOS.

A cosmological census shows that only 1% of the mass of the Universe is of known constitution.

Subject headings: White-dwarfs, Dark Matter, Cooling instabilities.

1. Introduction - Russell in England 1902–1905

After some time spent in attending lectures, Russell joined A. R. Hinks, a skilled observer, with whom he learned the techniques of accurate parallax determination. They used the Sheepshanks telescope, which cost[1] £3,183 in 1898. It was still at the Observatories for my early years in Cambridge, but was demolished in 1959. W. M. Smart, who used the telescope extensively, wryly remarked

> "It was a telescope of unusual design combining in a unique way the chief disadvantages of both the refractor and the reflector!"

[1]To turn these prices into current dollars, multiply by about 100

In 1903 Hinks was promoted to Chief Assistant at a salary of £220[1] per annum and a house provided. Russell's Carnegie (post doctoral) grant was £200[1] per annum.

It is a tribute to the persistence of Hinks and Russell that they eventually determined 50 parallaxes, many of which stand up well to comparison with modern determinations. A not atypical example is the parallax of the well known high velocity subdwarf Groombridge 1830 for which Russell gives $0.100 \pm 0.029''$ as compared to a modern value of $0.107''$. Thus, many of the stars in Russell's first HR diagram were put there on the basis of their Cambridge parallaxes.

2. Census of the Universe

The prediction that the angular wavelength of the first peak in the angular power spectrum of the cosmic microwave background would decide whether the Universe was closed or open was made only 14 years ago (Efstathiou & Bond 1986; Bond & Efstathiou 1987) [see also Doroshkevich et al. (1978)]. The first results of TOCO, Boomerang and Maxima are already with us. By contrast the prediction that many large galaxies including our own, M31, M32, M81, M82, M87, etc, contain giant-black-hole remnants of dead quasars in their nuclei (Lynden-Bell 1969) took over 26 years before the first definitive case was found (Miyoshi et al. 1995). Although there were indicative results earlier (Young et al. 1978; Sargent et al. 1978; Penston et al. 1981; Pounds et al. 1986; Dressler & Richstone 1988; Kormendy 1988) and many convincing ones since (Eckart & Genzel (1996); Genzel et al. (1997); Gebhart et al. (2000)). An interesting account of twentieth century developments is given in Shields (1999) review, but it can be argued that the first prediction was 211 years earlier (Michell 1784).

Astronomy is now running so fast that almost everything is as ephemeral as a news

report, nevertheless each entry in Table 1 is attested by at least two independent lines of evidence. For example, the cold dark matter fraction comes both from estimates of the baryon fraction in large X-ray emitting clusters of galaxies (White et al. 1993) and from estimates of the relative height of the peaks in the Maxima results. Likewise the unknown expansion energy estimate comes both from the difference between the closure density (TOCO, Boomerang and Maxima) and the total matter density of Maxima, **and** from the rate of acceleration of the Universe measured using distant supernovae.

However, if in a thought experiment we dream of reversing the Hubble expansion – but nevertheless leaving time running forward – then the black body radiation from the sky would get hotter and hotter. The white dwarfs, neutron stars and black holes would all survive to temperatures of more than 10^9K and there is then no time to destroy them before the big crunch. This thought experiment shows us that any compact bodies which might already be present at the time of Helium creation 10 seconds after the Big Bang would survive to the present day. If so, their baryons would not be counted in the first two entries but would contribute to the collisionless matter of the third entry. The two entries for baryons disagree but the second estimate is based on the results of Boomerang and Maxima which don't agree well either. Few believe the number of baryons goes up between 10 sec and 1/3 Myr and the first entry is considerably more secure. However, even that gives us a **missing baryon problem** because the numbers of baryons in stars, galaxies and intra-cluster gas is much less than that given by the first entry. Much may lie as yet undetected as 5.10^5 K gas in small groups of galaxies like ours. Detection of the dispersion measure to pulsars in the globular clusters of the Fornax dwarf would test this.

The wonder of astronomy lies as much in what is unknown as in the beauty of the 1% that is known. However, when discussing these unknowns, one should heed the wisdom of the past, so when lecturing about cold dark matter, I always quote

TIME	FRACTION $\Omega = \rho/\rho_c$		Ω
$H_o^{-1} = 10^{10} h^{-1}$yrs	$\rho_c = 3H_o^2/(8\pi G)$		$h = 0.6$
10sec	Baryons (Atoms)	$1.9h^{-2}\%$	5%
		± 0.1	
1/3 Myr	Baryons (Atoms)	$3.2h^{-2}\%$	9%
		± 0.6	
	Dark Matter + Baryons	$15h^{-2}\%$	40%
		± 5	
10^{10} yr	Radiation		0.007%
	Neutrinos		1% ?
	Unknown Expansion		
	Energy Ω_Λ (Supernovae)		$\sim 60\%$
1/3 Myr	Closure	1.03 ± 0.1	100%

Table 1: Universal constituents and effective times of measurements.

"If a thousand men believe a foolish thing it is still a foolish thing."

A new way of looking for invisible heavy halo objects via gravitational lensing events towards the Magellanic Clouds was first proposed by Petrou (1981). Independent calculations were made by Paczyński (1986), and it was he who stimulated Alcock et al. (1996) who first convinced the world that it was a practical possibility and led the Macho team to find such events (Alcock et al. 2000).

The Macho team found over twenty events toward the LMC which could account for between 10% and 20% of the Galaxy's dark halo, although almost half of the events might be self-lensing within the LMC. Whereas they found too few events to account for their halo model, both they and the Eros and Ogle teams found more than the expected number of lensing events towards the Galaxy's bulge. It would be not unnatural to imagine that the models of the Galaxy's mass distribution were seriously wrong with too little in the disc and too much in the halo, but that is not how the experts put it.

While pondering the nature of dark matter and the Macho results on Feb 15th 2000, I realised that there was a possibility that I had never heard discussed,

> "Could white dwarfs be made directly from primordial material without ever forming stars or burning hydrogen? Could such pristine white dwarfs be the halo objects found by Macho?"

As we shall see, such questions had occurred earlier to Salpeter (1992) and Hansen (1999).

3. Pristine and Halo White Dwarfs

Discussions of star formation often start with a large body contracting from a diffuse cloud. The equilibrium radius of such a body is determined by the Virial theorem.

$$\mathcal{T} = -\frac{1}{2}\mathcal{V} = -E \ ,$$

where $\mathcal{T}$ the kinetic energy is $\frac{3}{2}N k\bar{T}$ and $\mathcal{V}$ the potential energy is $-GM^2/(2\bar{R})$. The radiative loss from the surface causes the energy to get more negative so the radius $\bar{R}$ decreases and the internal temperature $\bar{T}$ increases until the nuclear reactions fire and the body becomes a star.

The above conclusion can be circumvented if the kinetic energy is not due to the star's temperature but is determined by the zero point energy of confined electrons required by the uncertainty principle. This occurs in solids and liquids.

If I were to freeze the A.A.S. President to absolute zero, she might become glassy eyed and she would shrink by an inch or so, but not substantially. This is because the electrons in her atoms owe their kinetic energy neither to their temperature nor to their angular momentum (since there is none in e.g., the ground state of hydrogen) but to their zero point degeneracy energy. They are of course held together by electricity.

Asteroids, planets and white dwarfs all owe their sizes to this zero point energy of electrons. In fact due to the work by Fowler (1926), Stoner (1929), Anderson (1929) and Chandrasekhar (1931) and by Salpeter (1967) in the 1960's, the mass radius relationship for such 'cold' bodies is one of the best understood parts of astrophysics.

In outline there are three terms:

- The zero point energy of the electrons which may or may not be relativistic.
- Their electrical binding to their associated atomic nuclei.

- The gravitational potential energy.

In small bodies such as asteroids, the main balance is between the zero point energy and the electrical attraction of the nuclei. Gravity merely serves to keep the parts together so as the bodies are piled together the mean density remains much the same. In spite of the increased pressure at the centre this equal density law still holds up to masses close to Saturn's. About there the gravitational binding starts to influence the total binding energy which is still mainly electrical. As a result the mean density starts to increase. At a mass a little over the mass of Jupiter gravitational and electrical binding become equal and the weight of each extra mass added causes a contraction as great as its volume. Beyond that point the bodies get smaller as the mass increases. When the zero point energy of each electron is substantially less than its rest mass, we get the brown dwarf–white dwarf sequence with $R \propto M^{-1/3}$. Once the electrons become relativistic the pressure generated becomes as soft as gravity and the radius decreases very rapidly as the Chandrasekhar mass is approached (Anderson 1929; Stoner 1930; Chandrasekhar 1931). It is possible to get a single mathematical formula for the whole mass-radius relationship from asteroids to Chandrasekhar's limit (Lynden-Bell & O'Dwyer 2001).

$$\left(\frac{4}{3}\pi\rho_0\right)^{1/3} R = \frac{M^{1/3}}{1+(M/M_p)^{2/3}} I \ ,$$

where M_p is the mass of the planet of maximum radius and ρ_0 is the density of the solid at zero pressure. I is unity except close to the Chandrasekhar limit M_{ch} where $I = J/[1+(3/4)(1-J^{1/2})]$ with $J = \sqrt{1-(M/M_{ch})^{4/3}}$.

The mass of the planet of maximum radius is set by the equality of gravitational and electrical attractions.

$$M_p \approx \left(\frac{e^2}{Gm_H^2}\right)^{3/2} m_H \ .$$

The Chandrasekhar mass is approximately $(\hbar c/e^2)^{3/2}$ times greater than this, showing that the fine structure constant plays a vital role.

In the theory of gravitational fragmentation the mass of the non-fragmenting fragment is given by (Low & Lynden-Bell 1976)

$$M = \left[\frac{3^5 \cdot 5^4}{2^8\pi^5}\left(\frac{\hbar c}{e^2}\right)\ \left(\frac{hc}{Gm_H^2}\right)^{10}\left(\frac{m_e}{m_H}\right)^2\right]^{1/7} m_H \simeq M_\odot/60\ ,$$

which may determine the minimum mass of bodies so formed, but as yet there is little evidence that nature pays too much attention! See in particular the fascinating σ Orionis Cluster (Zapatero-Osorio et al. 2000).

Figure 1 shows two mass-radius relationships; that on the left is appropriate for rock or for white-dwarfs with ($\mu = 2$) two baryon masses per electron. That on the right ($\mu = 8/7$) is appropriate for a pristine mixture of 75% Hydrogen and 25% Helium by mass, i.e., for Hydrogen planets, brown dwarfs and - if such exist - pristine white dwarfs. The latter have radii $R \propto \mu^{-5/3}M^{-1}$ that is 2.5 times larger than equal mass normal Helium, Carbon or Oxygen white dwarfs. At the same surface temperature we would expect them to be two magnitudes brighter. Since they have twelve times as many nuclei as Carbon white dwarfs their specific heats will be greater and they may not cool faster in spite of this extra emission.

When first interested in pristine white dwarfs I consulted early works by Parenago (1946) and by Eggen & Greenstein (1965) which showed two sequences separated by nearly two magnitudes. It was rather ironical to find that after Eggen consulted a theorist his work on the Hyades white dwarfs restricted itself to candidates within one magnitude of the expected sequence and would therefore have missed a second sequence. The idea was that in low-density regions such as cooling flows, galaxy haloes and dwarf spheroidals, stars form very gradually by accretion on to planetary sized seeds. If the growth was **so** slow that the accretion energy was radiated before the material was buried then the body would grow in mass resting on its zero point energy and never getting hot enough to fire its nuclear fuel.

When L-B raised the question of making pristine white dwarfs with C. A. Tout, his immediate reaction was that they would blow up like novae, but a day later he had found that novae only explode when the temperature of the degenerate hydrogen layer exceeds 10^6K. If the accretion rate were so small that the temperature never reached a million then pristine white dwarfs might be made.

To see if any had been observed we next consulted Mike Irwin. He said "it is possible that we have just what you are looking for" and sent us to read the growing literature on halo white dwarfs.

When Ibata et al. (1999) repeated the Hubble deep field three years later they found five objects at $29^{\rm th}$ magnitude which appeared to move. One may be a distant supernova in the side of a pre-existing image, two of the other images have unexpected asymmetries, but two looked like single stars[3] that move 20 milliarc sec/yr.

If such a star were brought 100 times closer it would be at $19^{\rm th}$ magnitude and move 2 arc sec/yr. Thus Irwin planned a wide–field Schmidt Survey to find such rapidly moving objects from existing plate material with plates taken less than ten years apart so that the faint stars would not move so far that they were 'lost' among others.

After searching over 700 square degrees Ibata et al. (2000) found 18 possible objects of which the brightest two were investigated spectroscopically. Both showed the strong infra-red blanketing predicted as the hallmark of molecular hydrogen formation in cool white dwarf atmospheres (Mould & Liebert (1978); Hansen (1998)). Both had motions

[3]Since this lecture was given, a third epoch HST frame has shown that neither of these remaining objects has a uniform motion, but the objects found by Schmidt surveys are real and more candidates have since been found (see Oppenheimer et al. (2001) and the criticisms of Reid et al. (2001)).

appropriate for halo stars 'left behind' by the rotation of the Galaxy. Earlier Hodgkin et al. (2000) had found another white dwarf showing the strong predicted infra-red blanketing. To be so fast moving and so dim the objects cannot be main-sequence stars without leaving the Galaxy. Making them old white dwarfs means they are quite close, about 30 parsecs. This means such objects are common; 50 times more common than earlier estimates of halo white dwarfs, but not all estimates (Chabrier et al. (1996); Chabrier (1999)) showed that if the halo mass function peaked a little above $1M_{\odot}$ then there could be many cool old white dwarfs. At such a density they would account for up to 10% of the dark halo. Others have objected that the population of heavier stars born with them would have produced more metals than are observed, but that would be avoided if these were pristine white dwarfs. At this juncture it seemed that the dark curtain over the nature of dark matter had let through a chink of light. L-B started to study how stars might form at low densities in cooling flows but, in the meantime, Tout was in real difficulties. Pristine white dwarfs over about $0.2M_{\odot}$ always fired their hydrogen unless their accretion rates were only 1 $M_{\odot}/10^{13}$ years – too slow to be made in this Universe. Furthermore this agreed with the estimates made by Salpeter (1992) on the basis of the accretion models of Lenzuni et al. (1992). Just as nuclear physicists predict an island of almost stable ultra-heavy nuclei that are very hard to make, so pristine white dwarfs between $0.2M_{\odot}$ and the cold pycnonuclear reaction limit of $1.1M_{\odot}$ are a theoretical possibility, but no-one knows how to make them!

This makes yet more interesting the origin of the large number of halo white dwarfs now being found. (See also Harris et al. (2001)).

4. Cooling Instability

Although the investigations of sections 4-7 were stimulated by the consideration of pristine white dwarfs, they are independent and develop the non-linear theory of cooling

instabilities which are probably important precursors of galaxy formation, star-cluster formation and normal star formation.

As stars are held together by gravity it is natural to believe that gravity is the primary driver in their condensation, but this may be wrong. At a density of 10^{-22}g cm^{-3} a solar mass of gas has an escape velocity of only 0.1 km/s whereas an ionised medium of that density will have a sound speed of about 10 km/s. At low densities pressure can be much more important than gravity and the pressure is often dictated by the cooling as the gas radiates to infinity (Fabian 1994).

Anyone who looks at photographs knows that the idea of a uniform interstellar medium is a theoretical abstraction far from truth. With such variations from place to place the cooling rate per gram will vary. This will induce pressure differences that will push the interstellar gas to the low pressure regions. The cooling is commonly such that regions of lower pressure have higher density. Thus condensations can form due to pressure alone, quite independently of any gravity. This is how condensation begins, the gravity comes in later.

We shall consider the simplest possible case of an optically thin gas at pressure p cooling by radiation to infinity. Suppose there are regions of different densities with anti-correlated temperatures so that dynamical equilibrium is maintained with the pressure spatially uniform. The second law of thermodynamics gives the entropy decrease consequent on the cooling $\rho^2\Lambda(T)$ per unit volume; so for unit mass

$$T\ Ds/Dt = -\rho\Lambda(T)\ . \tag{1}$$

For a perfect gas, $s = km^{-1}\ln(T^{3/2}/\rho) + \text{constant} = km^{-1}\ln(T^{5/2}/p) + \text{constant}$ where m is the molecular mass so for two regions of gas at a common pressure $p = m^{-1}kT\rho$,

$$(5/2)k^2m^{-2}p^{-1}D/Dt\ln(T_1/T_2) = T_2^{-2}\Lambda(T_2) - T_1^{-2}\Lambda(T_1)\ . \tag{2}$$

Hence as the gas cools the temperature ratio will increase whenever $T^{-2}\Lambda(T)$ is a decreasing function of temperature. This is the cooling instability criterion discovered by Fall & Rees (1985). As they pointed out it differs from the $T^{-1}\Lambda(T)$ decreasing criterion for thermal instability found in Field's masterly paper (Field 1965) and originally due to Weymann (1960). The reason for the difference is that Weyman and Field studied small departures from equilibrium conditions in which heating and cooling balanced in the mean state while the cooling instability criterion holds when everything is cooling on a timescale that is slow enough that the two regions share a common pressure (which may vary with time).

Figure 2, adapted from Dalgarno & McCray (1972), shows that for $30\mathrm{K} < T < 9000\mathrm{K}$ and $T > 10^4\mathrm{K}$ the whole range in which gas is ionised, $T^{-2}\Lambda(T)$ decreases. We deduce that in the absence of heating, cooling instabilities will occur and cooling condensations will develop. However, we have neglected two effects that work to suppress the instability. At small scales thermal conductivity will tend to suppress temperature differences and thus depress the instability by heating the denser regions. But, once the instability is kick started the thermal conductivity falls as the temperature falls so limiting the effect. More importantly Balbus & Soker (1989) have shown that, for infinitesimal perturbations, there are no thermal instabilities when the gas is in stratified equilibrium in a gravitational field. How can this be? Surely if we make the gravity field weaker and weaker we must arrive at the uniform medium instability criterion once the gravitationally induced gradients are weak enough! Here it becomes necessary to contrast mathematically exact results for infinitesimal perturbations with physical results for finite perturbations (Lufkin et al. 1995). An Astrophysicist might well consider a perturbation with $\delta\rho/\rho$ of 1/10 or even 1/3 to be quite small, but a Mathematician will consider only the limit as $\delta\rho/\rho$ tends to zero so that all its gradients are small compared with those that he has in his unperturbed state. For weak gravity fields this is a severe restriction on perturbation amplitudes especially at short wavelengths. We find in the next section that new density maxima caused by

the perturbation are all important. In an infinitesimal perturbation new density maxima only occur in a uniform medium. However small the gradient in the unperturbed state, infinitesimal perturbations make no new density maxima. For systems with a gravity field our results will only apply to finite amplitude perturbations which make new maxima.

5. Non-Linear Cooling Condensations

We take the simplest possible case of no external gravity, no self-gravity, no thermal conductivity and slow cooling so that the pressure is spatially constant. We consider this not because it is the most realistic case but because it gives insight and **insight** rather than complicated exactness is what science is about (Eddington 1926). Once the insight is obtained more complications are more readily understood. For a plasma cooling by free–free emission the cooling rate per gram can be written $\tilde{K}\rho c_s$ where c_s the sound speed is proportional to $T^{1/2}$. The coefficient $\tilde{K}$ has the dimensions $[M^{-1}L^4T^{-2}]$ which is one power of L more than the dimensions of G. As an aside it is interesting to ask how long this length $\tilde{K}/G$ is, since both free–free emission and gravity are inevitably involved in galaxy formation. In fact in fundamental dimensionless constants and the classical electron radius,

$$\tilde{K}/G = \frac{16}{3}\left(\frac{2\pi}{3}\,\frac{m_e}{m_p}\right)^{1/2}\left(\frac{e^2}{\hbar c}\right)\,\left(\frac{e^2}{Gm_em_p}\right)\frac{e^2}{m_ec^2} = 290 \text{ kpc} .$$

It is this large distance or rather 1/3.8 times it, that gives the 73 kpc radius from which galaxies fall together because their cooling rate is faster than their collapse time. We wish to discuss more general cooling laws but, although it is not hard to be more general, simplicity suggests a general power law $\propto \rho T^{2-\alpha}$ so the above case corresponds to $\alpha = 3/2$. With our general power law equations (1) and (2) together with the perfect gas law take the form

$$5/2\ D/Dt \ln\left(p^{3/5}/\rho\right) = -K\left(\rho/p^{3/5}\right)^{\alpha} p^{1-2\alpha/5} , \qquad (3)$$

so

$$D/Dt\left(p^{3/5}/\rho\right)^{\alpha} = -(2/5)\alpha K p^{1-2\alpha/5} \ . \tag{4}$$

Writing ρ_0 for the initial value of ρ on the fluid element considered and momentarily considering the special case with p independent of time we find

$$(p^{3/5}/\rho)^{\alpha} = (p^{3/5}/\rho_0)^{\alpha} - (2/5)\alpha K p^{1-2\alpha/5} t$$

and thence

$$\rho/\rho_0 = \left[1 - (2/5)\alpha K p^{1-\alpha}\rho_0^{\alpha} t\right]^{-1/\alpha} \tag{5}$$

However (4) may also be solved when p depends on time. We introduce a new weighted time τ defined by

$$\tau = \int (p/p_0)^{1-2\alpha/5} dt \ ,$$

where $p = p(t)$ and p_0 is its initial value.

Then in place of (5) we have the general solution

$$\rho/\rho_0 = (p/p_0)^{3/5}\left[1 - (\tau/\tau_c)\right]^{-1/\alpha} \ , \tag{6}$$

where $\tau_c = 5/(2\alpha K p_0^{1-\alpha}\rho_0^{\alpha})$ is the 'time' at which the density of our fluid element become formally infinite. With the Fall-Rees criterion satisfied $\alpha > 0$ so this time is shorter when the initial density ρ_0 is greater. Thus nucleation occurs around maxima in the initial density distribution. We rewrite (6) in terms of τ_m the collapse time for the initial density maximum ρ_m. Multiplying (6) by ρ_0/ρ_m we have

$$\rho/\rho_m = (p/p_0)^{3/5}\left[(\rho_0/\rho_m)^{-\alpha} - \tau/\tau_m\right]^{-1/\alpha} \ . \tag{7}$$

At time τ the current maximum density of the material whose initial density was ρ_m we call $\rho_c(\tau)$ or ρ_c for short. For the maximum density we put $\rho_0 = \rho_m$ in (7) and have

$$\rho_c/\rho_m = (p/p_0)^{3/5}|1 - \tau/\tau_m|^{-1/\alpha} \tag{8}$$

for $\tau < \tau_m$. Of course for $\tau > \tau_m$ the maximum density is infinite but we find it convenient to define ρ_c as a characteristic density given at all times by (8) even when $\tau > \tau_m$. This characteristic density is the maximum density at all times prior to $\tau = \tau_m$ and increases. After $\tau = \tau_m$ it becomes smaller again and represents the density at a self-similar point in the ensuing accretion flow. Dividing (7) by (8) we obtain

$$\frac{\rho}{\rho_c} = \left[\frac{(\rho_0/\rho_m)^{-\alpha} - 1}{|1 - \tau/\tau_m|} \pm 1 \right]^{-1/\alpha} , \tag{9}$$

where the plus sign is to be taken for $\tau < \tau_m$, before the centre collapses and the minus sign afterward. As $\tau \to \tau_m$ the denominator becomes small, so (9) is then very sensitive to small differences between ρ_0 and ρ_m. This means that the density profile near the collapse time τ_m depends solely on the initial profile of ρ_0 close to ρ_m. We now show how this leads to similarity solutions.

Let $M(> \rho_0)$ be initially the total mass, centred on one maximum of density ρ_m, which has at each point a density greater than some chosen value ρ_0. For a spherical density distribution around the maximum we have

$$dM = 4\pi r^2 \rho_0 dr = (dM/d\rho_0) d\rho_0 \ .$$

For a cylindrical distribution we replace $4\pi r^2 \rho_0 dr$ by $2\pi R \rho_0 dR$ while for a planar distribution we would replace it by $2\rho_0 dz$ and measure mass per unit area. Thus

$$\left.\begin{matrix} (4/3)\pi r^3 \\ \pi R^2 \\ 2|z| \end{matrix}\right\} = \int_{\rho_0}^{\rho_m} (\rho_0')^{-1} (dM/d\rho_0') d\rho_0' = \int_0^M [\rho_0(M')]^{-1} \, dM' \ , \tag{10}$$

where at the last equality we have used not $M(\rho_0)$ but its inverse function $\rho_0(M)$ which gives the density at the edge of the mass M of higher density. Now according to our cooling law higher densities get denser faster, so the density ordering of fluid elements remains the same. If a given initial density ρ_0 evolves into a density ρ after 'time' τ then the function

$\rho_0(M)$ will evolve into $\rho(M)$ with the **same** M. Thus the radius of the mass M at time τ will be given by analogy with (10) as

$$\left.\begin{matrix}(4/3)\pi r^3\\ \pi R^2\\ 2|z|\end{matrix}\right\} = \int_0^M 1/\rho(M')dM' \ . \tag{11}$$

Now near any smooth quadratic maximum the initial density takes the form

$$\rho_0 = \rho_m/(1+r^2/a^2) \equiv \rho_m(1+\alpha r^2/a^2)^{-1/\alpha} \ , \tag{12}$$

[where r^2 should be replaced by R^2 or z^2 for the $2D$ or $1D$ cases].

Hence

$$M = (4/3)\pi r^3\rho_m\left[1+O(r^2/a^2)\right] \ ,$$

so eliminating r in favour of M

$$\rho_0(M) = \begin{cases} \rho_m\left\{1+\alpha[3M/(4\pi a^3\rho_m)]^{2/3}\right\}^{-1/\alpha} & \text{spherical}\\ \rho_m\left\{1+\alpha M/(\pi a^2\rho_m)\right\}^{-1/\alpha} & \text{cylindrical}\\ \rho_m\left\{1+\alpha[M/(2a\rho_m)]^2\right\}^{-1/\alpha} & \text{planar}\end{cases} \tag{13}$$

Inserting this into (9) we find

$$\rho_0(M) = \left.\begin{cases}\rho_c(m^{2/3}\pm 1)^{1/\alpha}\\ \rho_c(m\pm 1)^{1/\alpha}\\ \rho_c(m^2\pm 1)^{1/\alpha}\end{cases}\right\} = \rho_c(\tau)\rho_*(m) \tag{14}$$

where

$$m = \begin{cases} 3\alpha^{3/2}M/(4\pi a^3\rho_m|1-\tau/\tau_m|^{3/2}) & \text{spherical}\\ \alpha M/(\pi a^2\rho_m|1-\tau/\tau_m|) & \text{cylindrical}\\ \alpha^{1/2}M/(2a\rho_m|1-\tau/\tau_m|^{1/2}) & \text{planar}\end{cases} \tag{15}$$

and

$$\rho_* = \begin{cases}(m^{2/3}\pm 1)^{-1/\alpha} & \text{spherical}\\ (m\pm 1)^{-1/\alpha} & \text{cylindrical}\\ (m^2\pm 1)^{-1/\alpha} & \text{planar}\end{cases} \tag{16}$$

To find r we insert (14) into (11) and deduce

$$(4/3)\pi r^3 \rho_c = \int_{0,M_c}^{M} (m^{2/3} \pm 1)^{1/\alpha} dM \tag{17}$$

where the lower limit is zero before collapse and the collapsed mass M_c afterward, as that collapsed mass does not contribute to the radius. Using the dimensional pieces of (15) and (8) to define a characteristic radius $r_c(t)$ we find $r = r_c(t) r_*(m)$ where

$$r_*^3 = \int_{0,1}^{m} (m^{2/3} \pm 1)^{1/\alpha} dm \ , \tag{18}$$

similarly

$$R_*^2 = \begin{cases} \frac{\alpha}{\alpha+1} \left[(m+1)^{1+1/\alpha} - 1 \right] & \tau \geq \tau_m \\ \frac{\alpha}{\alpha+1} (m-1)^{1+1/\alpha} & \tau \leq \tau_m \end{cases}$$

$$z_* = \int_{0,1}^{m} (m^2 \pm 1)^{1/\alpha} dm$$

where $R_* = R/R_c(t), z_* = |z|/z_c$ and

$$\begin{aligned} r_c(\tau) &= a|1 - \tau/\tau_m|^{1/2+1/3\alpha} \alpha^{-1/2} (p_0/p)^{1/5} \\ R_c(\tau) &= a|1 - \tau/\tau_m|^{1/2+1/2\alpha} \alpha^{-1/2} (p_0/p)^{3/10} \\ z_c(\tau) &= a|1 - \tau/\tau_m|^{1/2+1/\alpha} \alpha^{-1/2} (p_0/p)^{3/5} \end{aligned} \tag{19}$$

at least when p is constant.

$z_c(\tau) < R_c(\tau) < r_c(\tau)$ as τ approaches τ_m, and (19) always holds near $\tau = \tau_m$ since $p(\tau)$ is not sensitive to τ_m. Thus the planar collapse solution collapses fastest, just like the gravitational case. This strongly suggests that the spherical solutions are unstable to a flattening instability and we shall see that this is indeed true.

Equations (16) and (18) together constitute parametric equations for the density profile $\rho_*(r_*)$ in terms of the parameter m. From (14) it is already clear that the solution is self-similar both before and after the moment when the density first becomes singular. The spherical solutions with $\alpha = 1$ are plotted in Figure 3. This self-similarity rests on the

approximate form of ρ_0 close to its maximum ρ_m, so it only holds for times close to that moment. One may find $\rho_*(r_*)$, or rather its inverse function $r_*(\rho_*)$, explicitly for the special cases when $\alpha = 2/n$, with n an integer, but we keep to the general case and look at the asymptotic forms for small and for large r_*.

Pre-collapse

$$\left.\begin{array}{cc} \text{For } r_* \text{ small } r_*^3 = m + (3/5)\alpha^{-1}m^{5/3} & \text{so} \\ m = r_*^3 - (3/5)\alpha^{-1}r_*^5 & \text{and from (16)} \\ \rho_* \simeq (1+r_*^2)^{-1/\alpha} & r_* \text{ small} \end{array}\right\} \tag{20}$$

$$\left.\begin{array}{cc} \text{for } r_* \gg 1 & r_*^3 = \frac{3\alpha}{3\alpha+2}m^{2/(3\alpha)}\left[m + \frac{2+3\alpha}{2+\alpha}m^{1/3}\ldots\right] \\ & m = \eta^{-\eta}r_*^{3\eta}\left[1 - \frac{3\eta}{3+2\eta}\alpha^{-1}\eta^{1+2\eta/3}r_*^{-2\eta} + O(r_*^{-4\eta})\right] \\ \text{where} & \eta = 3\alpha/(3\alpha+2) \\ \text{so for large } r_*, \text{ (16) gives} & \rho_* = (1+\eta^{-2\eta/3}r_*^{2\eta})^{-1/\alpha} \propto r_*^{-6/(3\alpha+2)} \end{array}\right\} \tag{21}$$

Thus at the moment when the central density becomes singular we find a power law density profile with index $-6/(3\alpha+2)$. That is $-12/13$, $-6/5$ and $-12/7$ for $\alpha = 3/2,\ 1$ and $1/2$ respectively.

The $r^{-12/7}$ profile is the same as that for Penston's cold free-fall solution for a self gravitating spherical cloud, (Penston 1969).

Post collapse

$$\begin{array}{c} \text{For times later than } \tau_m \text{ the central point mass } M_c \text{ grows} \\ M_c = \left[(\tau/\tau_m) - 1\right]^{3/2}(4/3)\pi a^3\rho_m\alpha^{-3/2} \end{array} \tag{22}$$

which comes directly from expression (15) with $m = 1$. Of course (22) only holds when τ is close to τ_m when approximation (12) is valid. However, it is easy enough to determine $M_c(\tau)$ directly from the initial conditions. Let $M[\rho_0]$ be the mass within the ρ_0 density contour in the initial conditions and suppose it all has density $\geq \rho_0$ for all ρ_0 above some

minimum. Then from our expression for τ_c above (7) the mass that has collapsed by time τ is the mass that had initial density greater than $\left[(2/5)\alpha K p_0^{1-\alpha}\tau\right]^{-1/\alpha}$ i.e.,

$$M_c = M\left[\left((2/5)\alpha K p_0^{1-\alpha}\tau\right)^{-1/\alpha}\right] \tag{23}$$

Setting $m = 1 + \tilde{m}$ in (18), the post collapse similarity solution for times a little greater than τ_m is (see Figure 3c)

$$\begin{aligned} r_*^3 &= (2/3)^{1/\alpha}\left[\alpha/(\alpha+1)\right]\tilde{m}^{1+1/\alpha} + \ldots \\ \rho_*^{-\alpha} &= (2/3)\tilde{m} + \ldots \\ \text{hence}\quad \rho_* &= \left\{(3/2)\left[\alpha/(\alpha+1)\right] r_*^{-3}\right\}^{1/(\alpha+1)} + \ldots \quad \text{small } r_* \end{aligned} \tag{24}$$

i.e., a power law of index $-6/5,\ -3/2,$ or -2 for $\alpha = 3/2,\ 1,\ 1/2$. At $r > r_c(t)$ these power laws change over to the power $-6/(3\alpha+2)$ derived earlier.

6. Exactly Self-Similar Solutions

We derived these solutions as approximations, only good for times close to τ_m for regions not too far from the maximum density. However if, instead of postulating a general initial profile and then approximating it near maximum by (12), we had taken an initial profile defined by (18) and (16) then our solution would be exactly self-similar at all times and all positions. Perhaps the simplest of these is that given by Newton's law of cooling proportional to temperature. Then (18) integrates and yields for $\alpha = 1$

$$\begin{aligned} r_*^3 &= m + (3/5)m^{5/3} && \tau < \tau_m \\ & (3/5)(m^{5/3} - 1) - m + 1 && \tau > \tau_m \\ & \text{while (16) yields} && \rho_* = 1/(m^{2/3} \pm 1) \end{aligned}$$

Asymptotically $\rho_* \to r_*^{-6/5}$ for all large r_* so to keep the pressure constant $T \to r_*^{6/5}$.

Similarly the 'exact' solution for the cylindrical case gives ρ explicitly

$$\rho = \rho_c(t)/\left[U + (1+\alpha^{-1})R_*^2\right]^{1/(\alpha+1)}$$

where $U = 1$ for $\tau < \tau_m$ and 0 otherwise; $\rho_c(\tau)$ is still given by (8) in all three geometries.

For $\alpha = 1$ we have for the planar case

$$\rho_* = 1/(m^2 \pm 1)$$

$$\text{and} \quad z_* = |z|/z_c = \begin{cases} (1/3)m^3 + m & \tau < \tau_m \\ (1/3)m^3 - m + 2/3 & \tau > \tau_m \end{cases}$$

We have obtained all these solutions under the assumption that the cooling is so slow that we may take the pressure to be almost constant - i.e., the system evolves quasi-statically through a sequence of equilibria. Nevertheless if it evolves in finite time there must be small motions and very small accelerations to drive these small motions. To find these motions and the small pressure gradients that drive them we use the equations of fluid mechanics. By mass conservation

$$D\ln\rho/Dt = -\text{div } \mathbf{u} = -r^{-2}\partial/\partial r(r^2 u)$$

where u is the radial component of $\mathbf{u}$. We know $D\ln\rho/Dt$ from (3) so using (18)

$$u = -(1/5)(\dot{p}/p)r - (2/15)Kp^{1-\alpha}\rho_c^\alpha r_c r_*^{-2}\int_{0,1}^{m}(m^{2/3} \pm 1)^{(1-\alpha)/\alpha}dm \ .$$

When $\alpha = 1$ the final integral simplifies to m for $\tau < 0$ and $m - 1$ for $\tau > 0$. Such solutions are plotted for $\dot{p} = 0$ as Figure 4.

In $2D$

$$u = -(3/10)\,(\dot{p}/p)\,r - (1/5)Kp^{1-\alpha}\rho_c^\alpha R_c r_*^{-1}\alpha \begin{cases} (m+1)^{1/\alpha} - 1; & \tau < 0 \\ (m-1)^{1/\alpha}; & \tau > 0 \ . \end{cases}$$

In the planar case with $\alpha = 1$

$$u = -(3/5)(\dot{p}/p)z - (2/5)Kp^{1-\alpha}\rho_c^\alpha r_c m \ .$$

Notice that similarity only extends to the velocity fields when either $\dot{p}$ is zero or $\dot{p} \propto p^{2-\alpha}\rho_c^{\alpha}$. From the above Du/Dt, and thence the small pressure gradient can be calculated. Spherical self-similar solutions for the outer parts of cooling flows have been found numerically by Bertschinger (1989). His solutions are valid through the sonic region.

7. Flattening into Sheets

We saw in section 5 under (19) that the collapse time depended on the dimension and the planar collapse was fastest. We were thus led to believe that density maxima would flatten and the cooling instabilities would lead to curtain-like sheets of high density. To check that this is indeed the case, Marcus Brüggen, ran some 3D and 2D simulations. In these the full equations of fluid dynamics were integrated and the cooling was switched on over a few sound-crossing times to avoid transients. While the pressure was initially constant in space it was allowed to vary in space and time. While the cooling was slow it was not so slow that pressure remained constant and indeed it fell drastically in the cooling sheets that developed. Figures 5a and 5b which contour the density distribution initially, and after cooling, show clearly the development of flat sheets of high density just like those studied in planar geometry by Burkert & Lin (2000). The high density and low sound speed in these sheets make them ideal for gravitational instability and fragmentation into clusters of stars.

8. Conclusions

While some sort of census of the contents of the Universe is now possible, the true nature of the vast majority of it is unknown. Astronomy is still young.

Many more halo white dwarfs are now being found and this is likely to change our

concept of what the galaxy is like. They probably make a significant contribution to the dark matter (5% - 10%), however there remain serious doubts on the reality of this interpretation. This is an exciting and controversial subject that deserves our attention.

Pristine white dwarf configurations exist for objects that never burn hydrogen but no-one has devised a way of getting bodies to that state so the large numbers of halo white dwarfs now being found are probably normal burnt out stellar remnants.

Cooling instabilities may be the method by which density enhancements start in many different areas of astronomy; gravity may be only important in the final stages of star formation.

9. Acknowledgements

Firstly to the American Astronomical Society for the honour of asking L-B to give a Russell Lecture, the first of a new Millenium. Secondly to those who have been especially helpful; Marcus Brüggen using his expertise in simulating cooling clouds, M. J. Irwin, R. F. Griffin & F. van Leeuwen for their observations; and O. Lahav for Cosmological consultations.

Finally to Astronomy for the great fun it gives us all.

AAS ftp site. For technical support, please write to

aastex-help@aas.org.

REFERENCES

Alcock, C. et al. 1996, ApJ, 461, 84

Alcock, C. et al. 2000, ApJ, 542, 281

Anderson, W. 1929, Zsf Phys, 54, 433

Balbus, S. A. & Soker, N. 1989, ApJ, 341, 611

Barradoy-Navascues, D., Bailer-Jones, C. A. L. & Mundt, R. 2000, Science, 290, 106

Bertschinger, E. 1989, ApJ, 340, 667

Bond, J. R. & Efstathiou, G.P., MNRAS, 226, 655

Burkert, A. & Lin, D. N. C. 2000, ApJ, 537, 270

Chabrier, G., Segretain, L. & Méra, D. 1996, ApJ, 468, L21

Chabrier, G. 1999, ApJ, 513, L103

Chandrasekhar, S. 1931 ApJ, 74, 81 and 1931 MNRAS, 91, 456

Dalgarno, A. & McCray, R. 1972, Ann.Rev.Astron.Astrophys., 10, 375

Doroshkevich, A. G., Zeldovich, Y. A., & Sunyaev, R. A. 1978, Sov.Astr., 22, 523

Dressler, A. & Richstone, D. O. 1988, ApJ, 324, 701

Eckart, A. & Genzel, R. 1996, Nature, 383, 415

Eddington, A. S. 1926, The Internal Constitution of the Stars, Ch.72, p102, Cambridge University Press

Efstathiou, G. P. & Bond, J. R., 1986, Phil.Trans.R.Soc.London A, 320, 585

Eggen, O. J. & Greenstein, J. L. 1965, ApJ, 141, 83

Fabian, A. C. 1994, Ann.Rev.Astron.Astrophys., 32, 277

Fall, M. J. & Rees, M. J. 1985, ApJ, 298, 18

Field, G. B. 1965, ApJ, 142, 531

Fowler, R. H. 1926, MNRAS, 87, 114

Gebhart, K. et al. 2000, ApJ, 539, L13

Genzel, R., Eckart, A., Ott, T. & Eisenhauer, F. 1997, MNRAS, 291, 219

Hansen, B. M. S. 1998, Nature, 394, 860

Hansen, B. M. S. 1999, ApJ, 517, L39

Harris, H.C. et al. astro ph/0101021, ApJ Letters accepted

Hinks, A. R. & Russell, H. N. 1905, MNRAS, 65, 775

Hodgkin, S., Oppenheimer, B., Hambly, N., Jameson, R., Smartt, S. & Steel, I. 2000, Nature, 403, 57

Ibata, R., Richer, H., Gulliland, R. & Scott, D. 1999, ApJ, 524, 95L

Ibata, R., Irwin, M., Bienaymé, O, Scholz, R. & Guibert, J. 2000, ApJ, 532, 41L

Kormendy, J. 1988, ApJ, 335, 40

Lenzumi, J., Chernoff, D.F. & Salpeter, E.E. 1992, ApJ, 393, 232

Lin, D. N. C. & Murray, S. D. 2000, ApJ, 540, 170

Low, C. & Lynden-Bell, D. 1976, MNRAS, 176, 367

Lufkin, E. A., Balbus, S. A. & Hawley, J. F. 1995, ApJ, 446, 529

Lynden-Bell, D. 1969, Nature, 223, 690

Lynden-Bell, D. & O'Dwyer, J. P. 2001, astro-ph/0104450

Michell, J. 1784, Phil.Trans.R.Soc London, 74, 50

Miyoshi, M., Moran, J., Hernstein, J., Greenhill, L., Nakai, N., Diamond N. & Inoue, M. 1995, Nature, 373, 127

Mould, J. R. & Liebert, J. 1978, ApJ, 226, L29

Oppenheimer, B. R., Hambly, N. C., Digby, A. P., Hodgkin, S. T. & Saumon, D. 2001, astro-ph/0104293 (Science)

Paczyński, B. 1986, ApJ, 304, 1

Parenago, P. P. 1946, Astr.Zhur., 23, 31

Penston, M. V. 1969, MNRAS, 144, 425

Penston, M. V. et al. 1981, MNRAS, 196, 857-887

Petrou, M. 1981, Thesis Ch. VII pp 128-143, I.O.A. & Cambridge University Library

Pounds, K. A., Turner, T. J., Warwick, R. S. 1986, MNRAS, 221, 7p

Reid, I. N., Sahu, K. C. & Hawley, S. L. 2001, astro-ph/0104110 (ApJ letters submitted)

Russell, H. N. 1905, MNRAS, 65, 787

Salpeter, E.E., 1967, In Relativity Theory & Astrophysics, Vol. 3, Stellar Structure p, ed. J Ehlers, Lectures in Applied Mathematics, Vol 10, American Mathematical Science, Providence, Rhode Island

Salpeter, E. E. 1992, ApJ, 393, 258

Sargent, W. L. W., Young, P. J., Boksenberg, A., Shortridge, K., Lynds, C. R. & Hartwick, F. P. A. 1978, ApJ, 221, 731

Shields, G, 1999, Pub.Ast.Soc.Pac., 111, 661

Stoner, E. C. 1929, Phil.Mag., 7, 63

Stoner, E. C. 1930, Phil.Mag., 9, 944

Weymann, R.J., 1960, ApJ, 132, 380

White, S.D.M., Navarro, J.F., Evrard, A.E. & Frenk, C.S. 1993, Nature, 366, 429

Young, P. J., Westphal, J. A., Kristian, J., Wilson, C. P. & Landauer, F. P. 1978, ApJ, 221, 72

Zapatero-Osorio, M.R. et al. 2000, Science, 290, 103

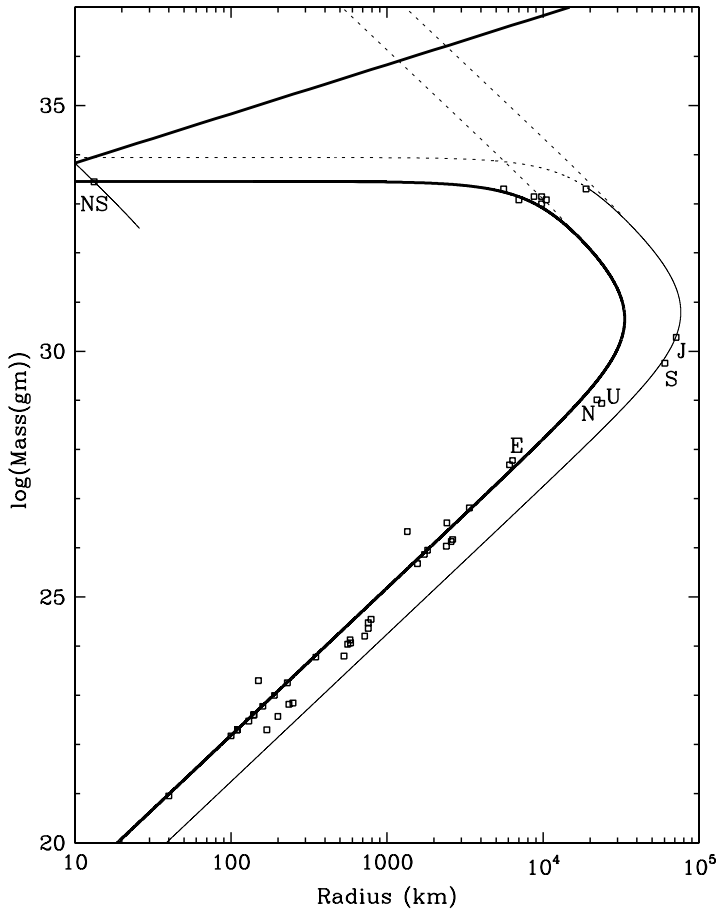

Fig. 1.— Figure 1. The heavy line on the left gives the mass-radius relation for cold bodies with $\rho_0 = 3.65$ g cm^{-3} and $\mu = 2$, suitable for rocky planets and normal white dwarfs. The heavy line above gives the black hole radius. The lighter line is for a mixture with 75% Hydrogen and 25% Helium, $\mu = 8/7$ suitable for gas-rich planets, brown dwarfs and pristine white dwarfs. This sequence ends at $1.1M_\odot$ due to pressure induced, (pycno-nuclear) reactions. Stable bodies could exist between 0.2 and $1.1M_\odot$ but no plausible formation path has been found. The dashed lines extrapolate the non-relativistic formula for degeneracy into the region of its invalidity. The neutron star line is parallel to these but displaced from the pure hydrogen line by the factor (m_e/m_n) in radius.

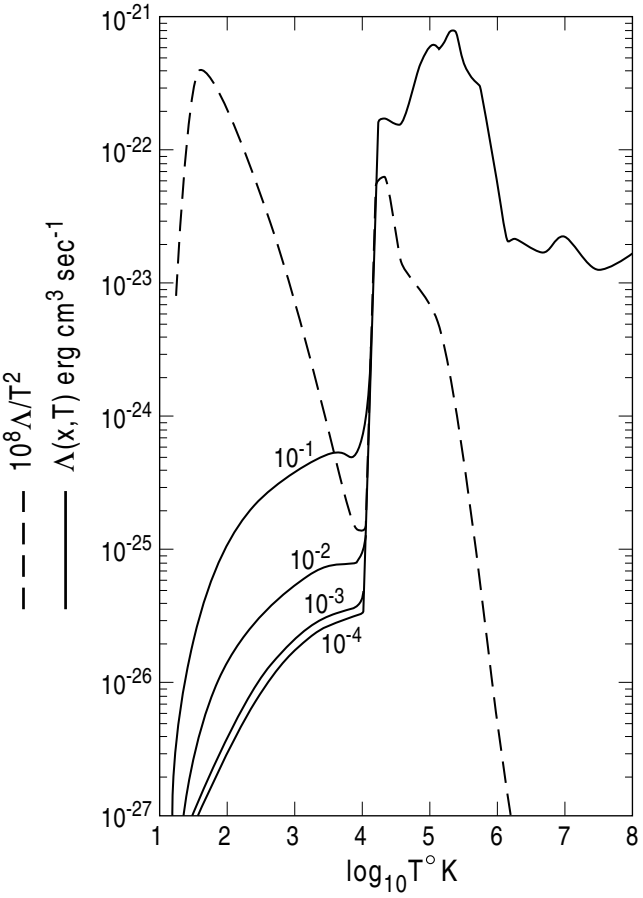

Fig. 2.— Figure 2. The cooling function $\Lambda(T)$ of Dalgarno &McCray with superimposed (dashed) the graph of $10^8\Lambda(T)/T^2$. There is cooling instability causing condensations in an otherwise homogeneous region wherever the latter graph is falling, i.e., everywhere with $T > 30K$ except the region near 10^4K where hydrogen is partially ionised. Cooling instability should be prevalent throughout astronomy.

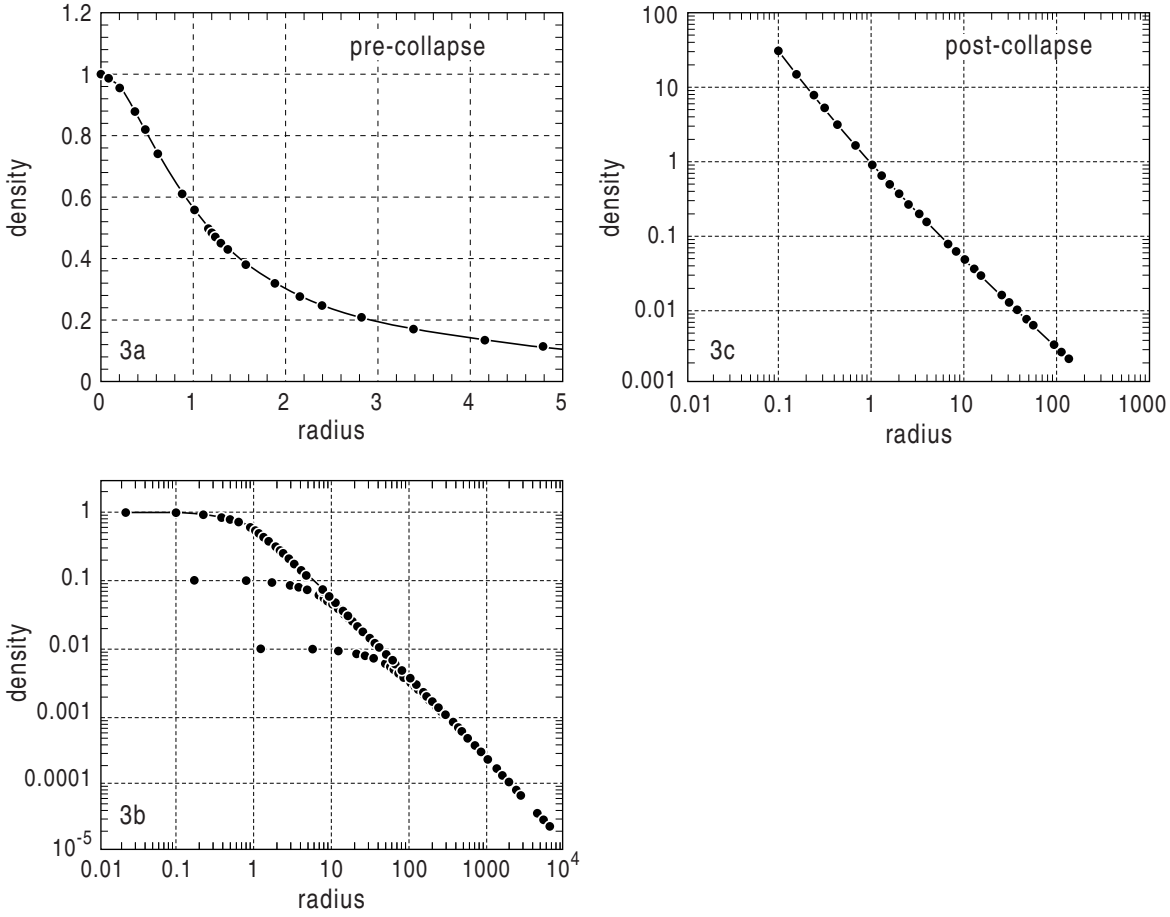

Fig. 3.— **Figure 3a**. The density profile for the spherical self-similar solution with $\alpha = 1$. **Figure 3b**. The log density – log radius profile at times $\frac{\tau}{\tau_m} = -1, -10, -100$ showing how the scale of the profile shrinks as $\tau = 0$ is approached. **Figure 3c**. The same as 3b but after the centre collapses. At $\tau = 1$ there is a growing central mass and the radius at which the power law changes from $-3/2$ to $-6/5$ increases like $(\tau/\tau_m - 1)^{5/6}$ again for $\alpha = 1$.

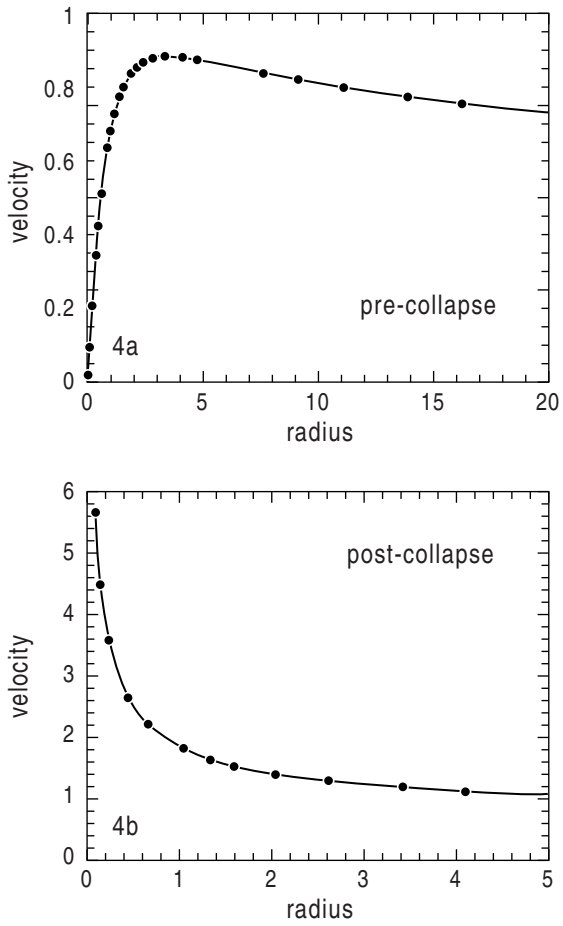

Fig. 4.— **Figure 4a**. The inward radial velocity profile prior to collapse of the core. **Figure 4b**. The same after the point mass develops $u \propto r^{-1/2}$ for small r and $u \propto r^{-1/5}$ for large r. The transition point moves outward.

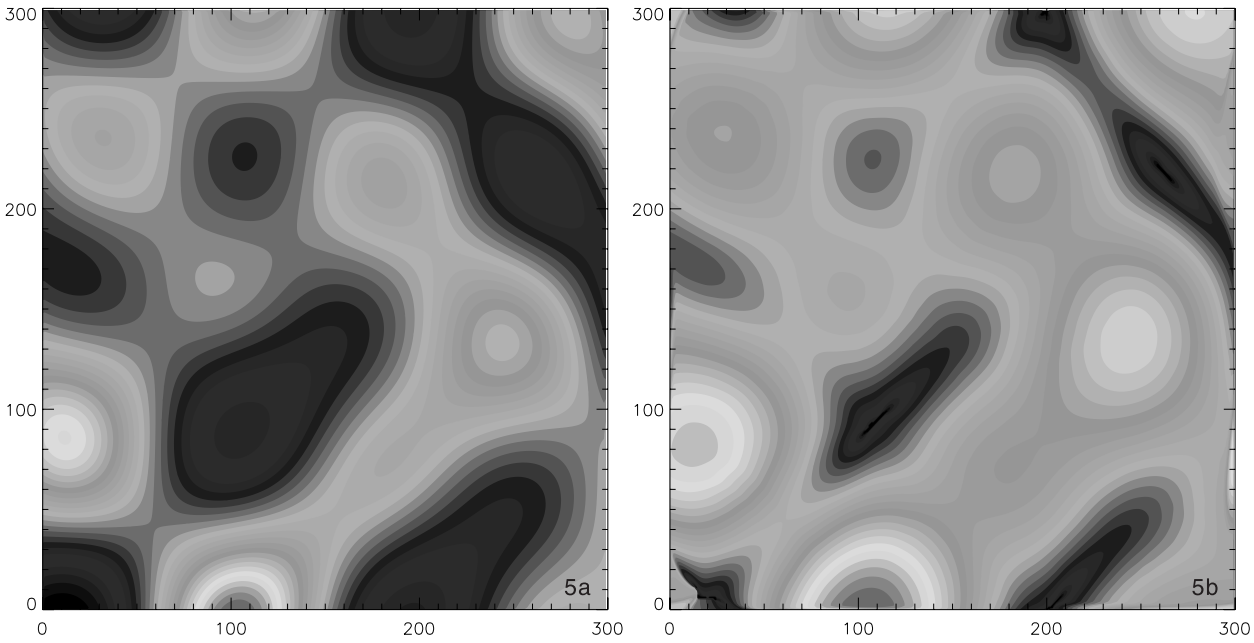

Fig. 5.— **Figure 5a**. Initial density contours of M. Bruggen's simulation of cooling flow. **Figure 5b**. Density contours after thin sheets develop which collect the mass.